Materials International
Open Access Journal (ISSN: 2668-5728)

Article
Volume 6, Issue 3, 2024, 24
https://doi.org/10.33263/Materials63.024

Adsorption, Thermodynamics, and Kinetic Studies on Beryllium Ions Removal from Aqueous Solutions by Amberlite XAD-2010 Resin Impregnated with Calcion

Wafaa Badawy [1], Walaa Hafez [1], Shaimaa Abdulmoteleb [1], Hayat El Agamy [1], Mohamed Atrees [1,*]

[1] Nuclear Materials Authority, P.O. Box 530, El Maadi, Cairo, Egypt; wafaa5.b@gmail.com (W.B.); walaasaeed12_h@yahoo.com (W.H.); shosho.salah22@yahoo.com (S.A.); Hayatrock97@hotmail.com (H.E.A.); msatrees@yahoo.com (M.A.);
* Correspondence: msatrees@yahoo.com (M.A.);

Scopus Author ID: 38361085700
Received: 11.03.2023; Accepted: 2.07.2024; Published: 10.09.2024

Abstract: Because of the many expected uses of beryllium from its ores in the future and the presence of exhausts resulting from its extraction, it was necessary to study how to remove these exhausts first. A novel, efficient beryllium adsorbent was prepared by impregnating calcion dye onto Amberlite XAD-2010 resin beads and characterized by FTIR and a scan electron microscope (SEM). Batch sorption experiments were carried out to remove beryllium from aqueous solutions using the new extractant-impregnated resin, EIR. The influences of various parameters such as pH, initial concentration, contact time, and the effect of temperature were evaluated. Optimum conditions for the maximum beryllium removal were performed at pH 3.5, with an equilibrium time of 25 min. The Langmuir sorption isotherm model better describes the equilibrium sorption isotherm. The thermodynamic data showed negative values of Gibbs free energy (ΔG), indicating that the sorption process was spontaneous at different temperatures. The entropy (ΔS) and enthalpy (ΔH) change were estimated. Results of the kinetic studies showed that the sorption process follows a pseudo-second-order model. To some extent, beryllium can be desorbed from the loaded resin using a 1.5 M HCl solution.

Keywords: beryllium; removal; adsorption; amberliteXAD-2010; calcion; equilibrium study, kinetic study.

1. Introduction

Beryllium (Be) is a unique strategic element due to its high importance and uses in several nuclear and non-nuclear industries. It doesn't appear as a free element in nature, and its presence is rather limited (6ppm) in the earth's crust. It is one of the lightest metals with high physical strength; it is about two-thirds as heavy as aluminum (Al) and has a modulus of elasticity of one-third greater than steel. So, it is a wonderful option to be a fundamental material in nuclear technology as a reflector, canning material, fuel diluent, and neutron source due to its lightweight and high melting temperature. Beryllium metal and its alloys have attracted much attention in various industrial applications such as electrical equipment, aircraft structural components, missiles, satellites, instrumental detectors, Geiger tubes, electrodes, computer parts,non-sparking tools, etc. It must be mentioned that Be is used in fabricating the X-ray windows because it transmits X-rays 17 times better than Al. Beryllium and its compounds exhibit extreme toxicity due to the inhalation of dust, fumes, or mists for susceptible individuals' health. Still, there is no evidence that it is toxic when handled (in

massive form). By far, there are about 40 minerals containing Be, but beryl Be_3Al_2 $(SiO3)_6$ is the most common Be mineral known in ancient Egypt as a gemstone (Emerald). Also, many German and British coal ashes contain a high Be content (0.1-1% Be) [1–4]. These applications prompted the development of various extraction methods and separation from different types of complex matrices, including precipitation, ion exchange [5], solid phase extraction [6], nano adsorbentextraction [7], hydrometallurgy and pyrometallurgyextraction [8], solvent extraction [9,10].

Among all currently available technologies, the adsorption method is convenient enough to be adopted in this study because of its low cost, environmentally friendly, and ease of operation for trace amounts of analyte from aqueous solutions compared to other methods with different adsorbents such as silica, metal oxide, zeolite, bentonite, modified chitosan, polystyrene, and activated carbon [5,11,12].

Recently, extractant-impregnated resins, EIRs, have been reported to be effective solid adsorbents for sorption and separating metal ions from their aqueous solutions. Metwally investigated the sorption of U(VI), Th(IV), and Co(II) ions from an acid medium using tri-dodecyl amine (TDA) loaded on a macroporous polymeric resin (XAD4)as a supporting material using the batch technique [13]. Navarro *et al*. prepared an extractant-impregnated resin (EIR) usedCyanex® 921 (tri-octyl phosphine oxide, TOPO) for the impregnation of Amberlite® XAD-7 [14]. Seyhan *et al*., used the impregnation of the polymeric matrix, Amberlite XAD-2000, with o-phenylenedioxydiacetic acid (OPDA) for the sorption of U(VI) and Th(IV) from aqueous solution [15]. Hosseini and Hosseini described a superior binding affinity for Th(IV) over U(VI) and many co-existing ions with eosin B and Amberlite IRA-410 resin [16]. Kovalenko *et al*. prepared solvent-impregnated resins (SIRs) by treatment of styrene–divinylbenzene copolymer (LPS-500) with mixtures of the promising polydentanteextractantdiphenylphosphine oxide (L) and an ionic liquid for the extraction chromatography of Nd(III) from nitric acid solutions [17]. Bezhin *et al*. investigated the physicochemical regularities of phosphorus and Be recovery by sorbents based on polyacrylonitrile (PAN) fiber and $Fe(OH)_3$ obtained by various methods [18]. Direct bonding of chelating ligands to a polymeric matrix is very difficult and time-consuming owing to the relative inertness of polymeric surface in the ground state; hence, surface activation is required. Therefore, the impregnation technique is the most convenient method of preparing chelating resins since it is exceedingly easy to perform. It merely requires stirring of the extractant and the polymeric support with a wide choice of reagents for the desired selectivity.

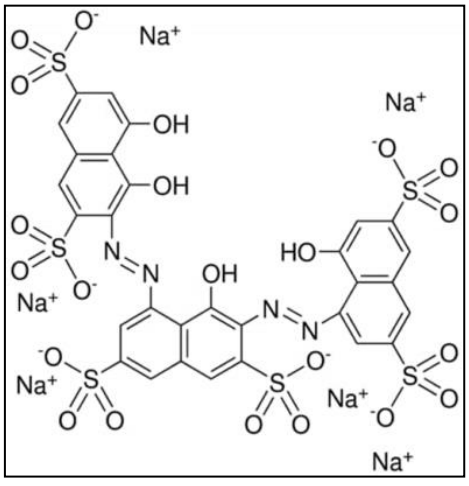

Figure 1. The structural formula of calcion dye.

In this study, the suggested resins (Amberlite XAD) found widespread application for separating and removing metal ions because they have good physical and chemical properties such as porosity, high surface area, durability, and purity [19,20]. Furthermore, the proposed reagent amino naphtholbisazo reactive dye (Calcion) ($C_{30}H_{14}O_{22}N_4S_6Na_6$) had three functional groups (one peri-hydroxy and two peri-orthodhydroxyazo), making it the preferred dye for this work. The structural formula of the calcion dye is presented in Figure 1 [21,22].

The addition of Be through waste drainage into natural bodies of water poses serious environmental hazards due to its high toxicity. Therefore, the current work is focused on designing an adequate chelating ion-exchange support for the sorption and removal of Be from aqueous solution, synthetic wastewater, and real industrial wastewater in small-scale effluent or low metal ion-contaminated industrial wastewater. For this purpose, calcion is impregnated onto the surface of Amberlite XAD-2010 resin beads to prepare a new extractant-impregnated resin, EIR. Batch sorption experiments examine the effectiveness of this EIR resin for the sorption of Be ion. To evaluate the effects of solution pH, contact time, initial concentration of Be ions, and temperature, batch sorption experiments are carried out using the optimum EIR sample. Thermodynamic parameters for Be sorption onto the new chelating ion-exchange resin are also estimated. In addition, the kinetic and equilibrium studies are used to gain insight into Be's potential sorption mechanism by EIR beads.

2. Materials and Methods

Materials and samples were provided by the Nuclear Materials Authority.

2.1. Chemicals and reagents.

All chemicals and reagents used in this study were of analytical grade. Beryllium stock solution (1000mgl^{-1}) was prepared by dissolving the appropriate amounts of beryllium sulfate trahydrate ($BeSO_4.4H_2O$), (Merck Co.) in deionized water. All the working solutions were prepared by diluting appropriate volumes from the stock solution with deionized water. Calcion dye (calcichrome) ($C_{30}H_{14}O_{22}N_4S_6Na_6$) and amberlite XAD-2010 were purchased from Sigma Co. Ethylene diamine tetraacetic acid disodium salt, EDTA-2Na (5%, w/v) ($C_{10}H_{14}O_8N_2Na_2$. 2H2O) supplied from Adwick Co. was prepared by dissolving 5g of analytical grade in double distilled water and diluted in 100ml volumetric flask and hydrochloric acid (1.5M HCl), purchased from Merck Co.

2.2. Instruments

Spectrophotometric measurements were performed by using a double beam UV–Visible spectrophotometer of high-resolution power model Jasco V-530 with a wavelength ranging from 190 to 1100 nm; computer controlled data analysis and reporting software was used in the systematic study to determine Be. The pH value was controlled by using a Jenway pH meter.

Morphological characteristics of EIR before and after the adsorption of Be ions were investigated by scanning electron microscope (SEM) (Philips XL 30, Holand). Absorption spectra in the IR region were recorded using a Fourier transform infrared spectrometer (FTIR) on the wave number range 4000– 400cm^{-1} (Thermo Scientific, NICOLET IS10, USA) used to characterize the major functional groups of the sorbent.

2.3. Preparation of the EIR.

An adsorbent preparation was carried out by using manufactured beads for impregnation. Consequently, when using these beads, many impurities must be eliminated. So, the Amberlite resin XAD-2010 was treated with 1:1 methanol and HCl (50ml of methanol: 50ml of 6M HCl) for 12 hours to remove any impurities or unwanted particles. The resin was rinsed with double-distilled water and placed into a drying oven at 50°C for 30 minutes. To prepare the impregnated resin, 1g of dry Amberlite XAD-2010 resin was transferred into a glass stoppered bottle containing 1g of calcion in 200 ml methanol, which was utilized as the solvent. The content was slowly shaken for 6h to accomplish the impregnation process and then was placed into a drying oven to expel the solvent at 50°C. The EIR sample was then transferred to a filter paper and washed consecutively with 3M HCl and large volumes of distilled water until no dye escaped into the filtrate. Finally, the impregnated resin was dried at 50°C and weighed [23].

2.4. Sorption procedures.

A batch technique was used to sorb the Be ions at room temperature. Aliquots of aqueous solution containing suitable concentrations of Be were taken in glass-stoppered bottles and adjusted to a known pH. The EIR beads (0.05g) were added to each bottle, and the mixtures were equilibrated for a specified period. The EIR beads were filtered, and the sorbed Be ions were desorbed by shaking with 1.5M HCl. The desorbed ions were measured spectrophotometrically by chrome azurol S procedure [1].

The sorption isotherms of Be ions onto the EIR were obtained at the pH of maximum uptake. For this purpose, aliquots of the solutions (pH 3.5) containing Be with the different concentrations were shaken at 25 ± 1℃ for 25min. These experiments were performed at various temperatures to obtain thermodynamic data.

For sorption kinetic data, a series of fixed-weighed portions (0.05g) of the EIRs were immersed into vessels containing aliquots of Be (pH 3.5) with a concentration of 1.1×10^{-4} M. The mixtures were shaken at ambient temperature for different time intervals. Portions of the supernatant were withdrawn from the solutions and subjected to the determination processes.

The amounts of metal ions adsorbed per gram of the EIR beads were calculated at equilibrium (q_e) and at various time‘t’ (q_t) by the difference between the initial and the final readings using the following equations.

$$\mathbf{q_e} = \frac{(\mathbf{C_0}-\mathbf{C_e})\mathbf{V}}{\mathbf{m}} \quad (1)$$

$$\mathbf{q_t} = \frac{(\mathbf{C_0}-\mathbf{C_t})\mathbf{V}}{\mathbf{m}} \quad (2)$$

Where *qt* is the amount of Be ions adsorbed onto the EIR beads at variable time t (mg g^{-1}), q_e is (adsorption capacity) the amount of the ions sorbed onto the EIR beads at equilibrium (mg g^{-1}), C_0 is the initial concentration of Be in the aqueous solutions (mg l^{-1}), C_t is the remaining concentration of Be in the solutions at time t (mg l^{-1}), C_e is the equilibrium concentration of Be (mg l^{-1}), *V* is the volume of the solutions used by the liter, *m* is the weight of the EIR beads used in gram and *(R%)* is the removal percentage at equilibrium was calculated by equation (3) [24].

$$\mathbf{R\%} = \frac{(\mathbf{C_0}-\mathbf{C_e})}{\mathbf{C_0}} \times \mathbf{100} \quad (3)$$

3. Results and Discussion

3.1. Sorbent characterization.

The FTIR spectra of Amberlite XAD-2010 before and after impregnation are shown in Figure 2. The IR spectrum of Amberlite XAD-2010 resin exhibits a less intense band at 3412 cm^{-1}, which can be attributed to the O-H stretching vibration of interlayer water molecules [25]. The bands between 3019 and 2923cm^{-1} are related to the stretching modes of the aromatic and aliphatic C–H groups. There are bands between 1617 and 1421cm^{-1} that are assigned to the vibration of benzene rings, which also contain contributions due to the bending modes of the methyl and methylene groups, and the bands observed at 923, 860, 828, and 707cm^{-1} are attributed to out of plane ring C–H bending vibrations [26]. Upon impregnation with calcion, a medium band around 3427cm^{-1} is ascertained to be OH of the phenolic group. The peaks observed at 1380 and 1420cm^{-1} are ascribed to C-N and N=N stretching vibrations, respectively [27]. Moreover, the stretching vibrations of the S =O and SO_3^{2-} are observed at 1038, 1218, and 1119cm^{-1}, respectively [28,29]. Furthermore, it is noticed that the characteristic bands related to the polymeric skeleton are present in the impregnated resin spectrum with a slight shift (5-10cm^{-1}), which confirms that the impregnation process has been performed through a physical sorption pathway.

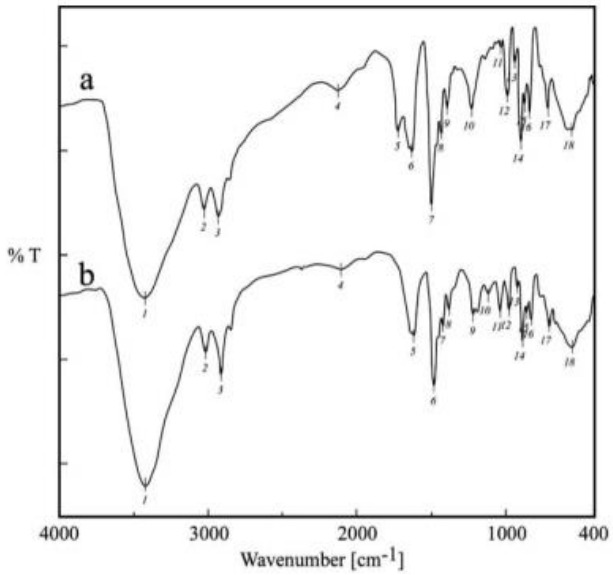

Figure 2. FTIR spectroscopy of the working polymeric resin: **(a)** Amberlite XAD-2010; **(b)** calcion /XAD-2010 modified resin.

3.2. Effect of pH.

pH is one of the most essential operational parameters in adsorption experiments, as it determines the nature of the metal ions and the sorbent's surface properties. Batch sorption studies were performed to investigate the influence of pH on the sorption of Be onto calcionXAD-2010 from aqueous solutions in which the pH of the working solution was varied from 1.0 to 8.0 at room temperature. According to the obtained experimental data in Figure 3, the separation of Be ions from the aqueous phase is completely pH-dependent. It was found that the removal of Be increases with increasing the pH from 1.0 to 3.0 and reaches a maximum value at the pH range of 3.0-5.0; then, as the pH increases, the removal percentage decreases. The possible reason for the decrease above could be precipitation phenomena at higher pH

[30]. Beryllium exists as the tetra-hydrated ion [Be $(H_2O)_4]^{2+}$ in an acidic solution (pH 1-4). While at pH above 5, the precipitation of Be ions as Be $(OH)_2$ was observed. Hence, pH 3.5 was selected for further optimization studies to remove Be ions [31].

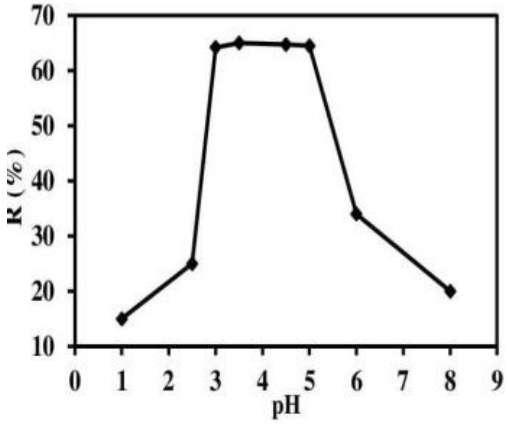

Figure 3. Effect of pH on the removal percentage of Be by EIR resin.

3.3. Effect of initial beryllium concentration.

Studying metal concentration is important for metal removal from its aqueous solution. Therefore, the effect of initial metal concentration is of significance in adsorption studies since it depends on several parameters, such as the type of metal and the liquid medium, the availability of the functional groups in the adsorbent surface, and the ability of these groups to attach metal ions [32]. To investigate the effect of initial beryllium concentration upon the removal percentage of the modified Amberlite XAD-2010 resin, a series of experiments were performed by contacting a fixed weight (0.05g) for a certain time at room temperature. The obtained results are plotted in Fig.4. From this figure, it is obvious that the Be removal percentage decreases with increasing its initial concentration. The adsorption of Be ions was studied at lower concentrations due to their detrimental and toxic consequences. This may be because, at lower initial concentration, the ratio of metal cations to EIR resin mass is low; a rise in initial concentration implies that additional metal ions are present in the mixture, and hence, more ions are attached to the same quantity of the resin which results in saturation of the adsorbent causing a decrease in R % [33].

The infrared technique was used for further study of the adsorption mechanism, Fig.5. Comparing both spectra of EIR before and after adsorption, there is a noticeable change in the spectra of the EIR resin from that of EIR loaded with Be in terms of position, shapes, and intensities. After adsorption, the band noticed at 1380cm^{-1} corresponding to (C-N) stretching vibration for EIR is shifted to 1113cm^{-1}. In addition, the band that was observed at 1420cm^{-1} due to (N=N) stretching vibration is shifted to 1377cm^{-1}. Also, the bands at 1119, 1038 cm^{-1} of the SO_3^{2-} and S =O are shifted to 979, 888cm^{-1}. The appearance of bands in 618cm^{-1} and 458cm^{-1} are assigned to υ (M-N) and υ (M-O) stretching vibration [34]. The shifts and changes in band frequencies indicate that the beryllium ions have been coordinated with EIR resin.

On the other hand, the scanning electron microscope (SEM) is considered the most reliable and convenient tool for studying the physical structure of the synthesized EIR resin beads. Therefore, to demonstrate the morphological features and the surface characteristics of the synthesized resin before and after Be sorption, the corresponding SEM micrographs are shown in Figure 6. As seen in Fig. 6a, the appearance of EIR resin before adsorption is uniform

and smooth. Meanwhile after adsorption, brilliant spots are observed on the resin beads, as shown in Figure 6b.

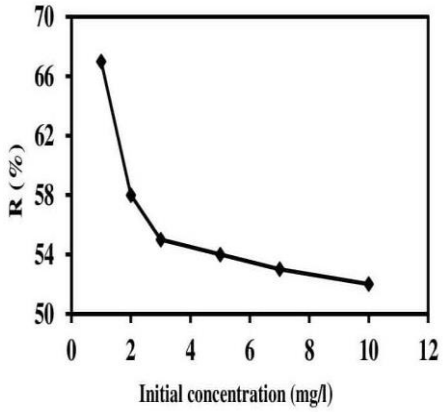

Figure 4. Effect of initial concentration on the removal percentage of Be by EIR resin.

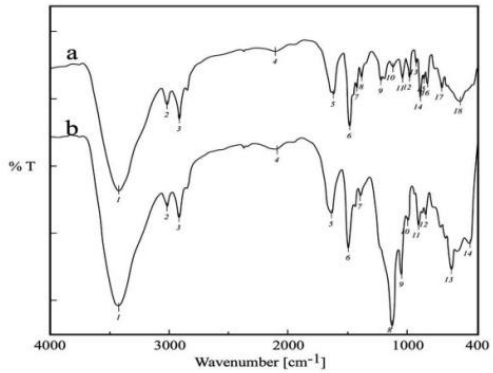

Figure 5. FTIR spectroscopy of **(a)** EIR resin; **(b)** Be loaded EIR resin.

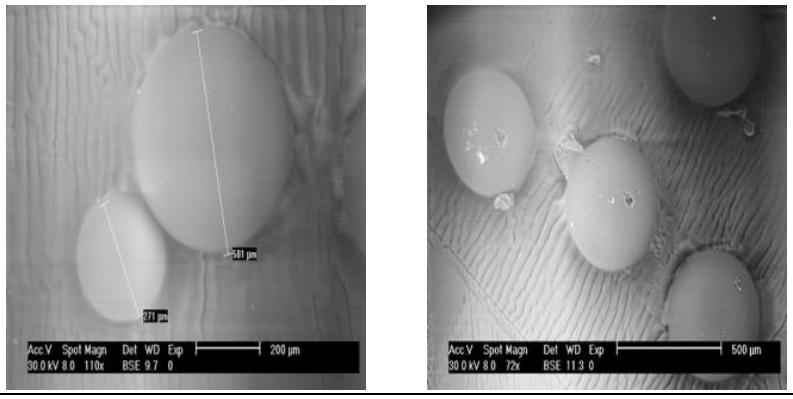

(a) **(b)**

Figure 6. SEM images of **(a)** EIR resin; **(b)** Be-loaded EIR resin.

3.4. Adsorption equilibrium studies.

Generally, solute encounters a finite distribution between the liquid and solid phases at the sorption equilibrium, which a variety of isotherms can describe, and adsorption models can be used to fit the observed experimental data and determine the model parameters. The sorption isotherm is a functional expression that relates the amount of solute adsorbed per unit weight of the adsorbent and the solute concentration in bulk solution at a particular temperature under equilibrium conditions. Moreover, it is an important physicochemical property for estimating an 'adsorbent's sorption capacity and energy [26].

To investigate the best model of adsorption, exact weighed portions of 0.05g of EIR resin were contacted with a series of solutions containing different concentrations of Be at pH 3.5 for 25 minutes. The maximum adsorption capacity of the investigated adsorbent is 2.75mg Be per gram of EIR resin. Several isotherm models were used to treat the data from the adsorption experiments (Langmuir, Freundlich, Temkin, and Dubinin-Radushkevich).

Langmuir proposes that adsorption is a monolayer system at a homogeneous adsorbent surface with energetically similar adsorption sites. It also presupposes that sorption occurs as a monolayer at the surface of the sorbent [35,36].

The linear form of Langmuir isotherm model is represented by the following equation:

$$\frac{1}{q_e} = \left(\frac{1}{q_m K_L}\right)\frac{1}{C_e} + \frac{1}{q_m} \qquad (4)$$

Where C_e is the equilibrium concentration (mg l^{-1}), q_e is the adsorption capacity at equilibrium (mg g^{-1}), q_m represents the monolayer capacity (mg g^{-1}), and K_L is the Langmuir constant related to the energy of adsorption (l mg^{-1}). A linear plot of $1/q_e$ versus $1/C_e$ based on the data obtained from the batch tests is given in Figure 7. From the plotted linear relation, the sorption values and correlation coefficients for Be sorption on the prepared EIR resin are recorded in Table 1.

A dimensionless constant called equilibrium parameter or separation factor, R_L, can be used to predict whether a sorption system is favorable or unfavorable. This parameter is evaluated from the essential characteristics of the Langmuir equation and can be calculated by the following equation:

$$R_L = \frac{1}{1+K_L C_i} \qquad (5)$$

Where C_i is the initial Be concentration (mg l^{-1}). The value of R_L indicates the nature of the isotherm to be irreversible (R_L= 0), favorable (0 < R_L< 1), linear (R_L=1), and unfavorable (R_L> 1) [37]. From the obtained data, the prepared EIR resin appears to be a favorable sorbent for Be since the R_L value is between 0 and 1.

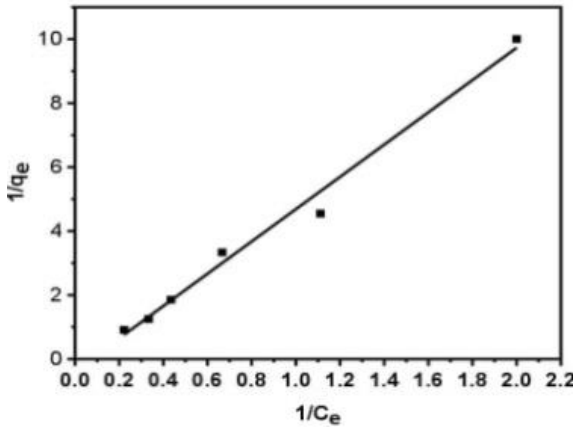

Figure7. Langmuir isotherm for the adsorption of Be by EIR resin.

Lu *et al.*and Freundlich [36, 38] (isotherm) suggest that the adsorption occurs on a hetero generous surface by a multilayer system in a linear form, as:

$$\log q_e = \log K_F + \frac{1}{n}\log C_e \qquad (6)$$

Where K_F and n are the Freundlich constants, which represent sorption capacity and sorption intensity, respectively. The values of Freundlich constants are calculated from the slope and intercept of the log q_e versus log $C_e$plot (Figure 8) and are listed in Table 1. It was

found that 1/n lies between zero and one; this indicates a favorable sorption process [39]. The value of the regression coefficient was lower than the Langmuir isotherm value. Therefore, the linear form of the Langmuir isotherm appears to produce a reasonable model.

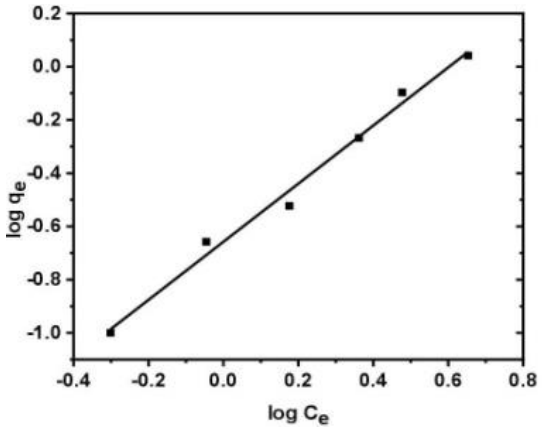

Figure 8. Freundlich isotherm for the adsorption of Be by EIR resin.

The Temkin isotherm model supposes that the adsorption heat of all molecules decreases linearly with increasing surface adsorbent coverage. That adsorption is characterized by a uniform distribution of binding energies up to a maximum binding energy. It can be depicted by Equation (7) [40,41].

$$\mathbf{q_e = B_T ln A_T + B_T ln C_e} \qquad (7)$$

$$\mathbf{B_T = \frac{RT}{b_T}}$$

Where A_T is the equilibrium binding constant (L g^{-1}) corresponding to the maximum binding energy, b_T is the Temkin isotherm constant, B_T is the adsorption heat constant, R is the universal gas constant (8.314Jmol^{-1}K^{-1}), and T is the temperature (K) A plot of q_e vs. lnCe enables the determination of isotherm constants B_T and A_T from the slope and the intercept, respectively (Table 1). The small value of A_T indicates the physical binding between the beryllium ion and EIR resin active sites (physisorption mechanism). Moreover, the value of B_T is lower than 8kJmol^{-1}, which indicating the sorption process is a physical adsorption process [39].

Another equation used in the analysis of isotherms was proposed by Dubinin and Radushkevich [42]. The D–R isotherm is expressed in the linear form as the following equation:

$$\mathbf{ln q_e = ln q_s - \beta \varepsilon^2} \qquad (8)$$

Where q_s refers to the theoretical saturation capacity (mg g^{-1}). β is the Dubinin–Radushkevich isotherm constant (mol^{2}kJ^{-2}), and ε is the Polanyi potential, which depends on temperature and equilibrium concentration of metal ion and is given by Equation (9).

$$\mathbf{\varepsilon = RT ln\left(1 + \frac{1}{C_e}\right)} \qquad (9)$$

To demonstrate the mechanism of the sorption process, the mean free energy (E) of the adsorption process was computed using the following relationship:

$$\mathbf{E = \frac{1}{\sqrt{2\beta}}} \qquad (10)$$

From the obtained data in Table 1, the value of E is less than 8kJmol^{-1}for Beions, implying that the adsorption process proceeds via physisorption [38]. Values of q_s and β can

be determined through linearization of the D-R isotherm. Plotting $\ln q_e$ versus ε^2, using Equation (8), results in a straight slope line β and intercept ln q_s (Figure 9).

Considering the results obtained from the four models, it is realized that the sorption process obeys the Langmuir model due to the higher correlation coefficient and a better fit to adsorption data than the other isotherm equations. This explains the Langmuir model's suitability for describing Be's adsorption onto EIR resin.

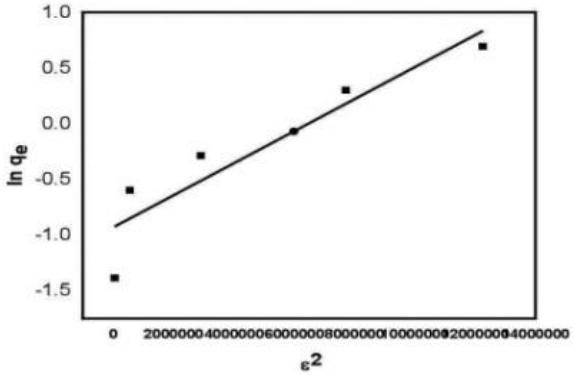

Figure 9. The Dubinin- Radushkevich (D-R) isotherm model of Be adsorption by EIR resin**.**

Table 1. The isotherm parameters for the adsorption of Be on EIR resin.

Isotherm model	Parameters	Value
Langmuir	qmax	2.75 mg/g
	KL	0.25
	RL	0.4
	R2	
Freundlich	KF	0.301
	n	1.5
	R2	0.9355
Temkin	BT	1.1
	AT	1.9
	R2	0.8927
D-R	β	1.5
	E	0.6
	R2	0.8606

3.5. Effect of contact time and kinetics studies.

To study the effect of contact time on the removal of Be by the EIR resin, aliquots of 25 ml of the solutions (pH 3.5) containing a fixed concentration of Be were shaken at 25°C for different time intervals (5- 40min) using 50mg resin. As illustrated in Figure 10, the removal amount of Be increased with increasing time and attained equilibrium at 25min. Therefore, 25 min of contact time was recommended in the present work.

The kinetic models give important information for designing the sorption process for Beremoval from its solutions, as well as predicting the sorption rate. To determine the kinetics of the sorption process of Be onto EIR resin, different kinetic models, including pseudo-first-order, pseudo-second-order, and intra-particle diffusion models, are used to investigate the sorption kinetic process.

The equations of pseudo-first-order and pseudo-second-order models are given as follows [43, 44]:

$$\ln(q_e - q_t) = lnq_e - K_1 t \quad (11)$$

$$\frac{t}{q_t} = \frac{1}{K_2 q_e^2} + \frac{t}{q_e} \quad (12)$$

Where q_e and q_t (mg g^{-1}) are the amounts of Be sorbed at equilibrium and at time t (min), respectively, k_1 (min^{-1})and k_2 (g mg^{-1} min^{-1}) are pseudo-first-order and -second-order

sorption rate constants, respectively.Kinetic parameters of these models were calculated from the slope and intercept of the linear plots of ln (q_e- q_t) versus t (Figure 11), t/q_t versus t (Figure 12), and given in Table 2.

Based on the correlation coefficients (Table 2), the pseudo-second-order kinetic model has provided a good correlation for the Be sorption. Additionally, there was a close agreement between the theoretical and the experimental values of q_e, confirming the validity of the pseudo-second-order model to elucidate the Be sorption mechanism by the prepared EIR resin.

The kinetics data was also used to analyze the intra-particle diffusion for the adsorption of Be ions on the prepared resin. This approach was based on the Weber and Morris model [45]. The model was characterized by the following equation:

$$\mathbf{q_t = K_{id}^{0.5} + C} \qquad (13)$$

Where q_t (mg g^{-1}) is the Be adsorbed amount at time t, K_{id} (mg g^{-I} $min^{-0.5}$) is the intra-particle diffusion rate constant, and C is the thickness of the boundary layer. According to this model, the plot of uptake (q_t) versus the square root of time ($t^{0.5}$) should be linear if intra-particle diffusion is involved in the adsorption process. If these lines pass through the origin, then intra-particle diffusion is the rate-controlling step. When the plots do not pass through the origin, this is an indication of some degree of boundary layer control, and the intra-particle diffusion is not the only rate-limiting step, but also other kinetic models may control the sorption rate, all of which may be operating simultaneously [45].

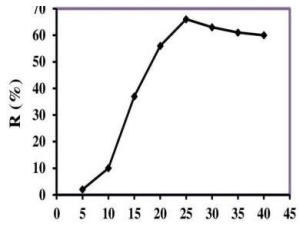

Figure10. Effect of contact time on the removal percentage of Be by EIR resin.

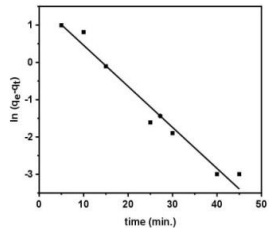

Figure 11. Pseudo-first-order kinetic of Be adsorption by EIR resin.

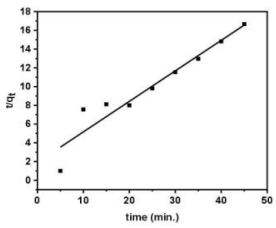

Figure 12. Pseudo-second-order kinetic of Be adsorption onto EIR resin.

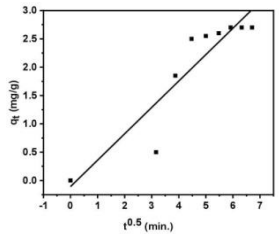

Figure13. Intra-particle diffusion model plot ForBe adsorption by EIR resin.

The intra-particle diffusion parameters are obtained from the linear plot's slope and intercept, as represented in Figure 13. The plot of q_t vs. $t^{0.5}$ gives a straight line that does not pass through the origin (C > 0). From the presented data in Table 2, it was noticed that the value of correlation coefficient R^2 is 0.842 while the intra-particle diffusion rate constants K_{id} is 0.46mg g^{-1} $min^{-0.5}$, and the thickness of the boundary layer C is 0.1mg g^{-1}. Therefore, in view of these data, it can be said that the intra-particle diffusion kinetic model is not appropriate for describing the sorption kinetics. Ultimately, from the kinetic parameters of three kinetic models, as seen in Table 2, the adsorption kinetics is estimated and fitted well by the pseudo-second-order kinetic model.

Table 2. The kinetic parameters for the adsorption of Be on EIR resin.

Pseudo-First-order			
q_e (mg g^{-1})	**K_1 (min^{-1})**	**R^2**	**Exp. q_e (mg g^{-1})**
4.71	0.002	0.9174	2.75
Pseudo-Second-order			
q_e (mg g^{-1})	K_2 (g mg^{-1} min^{-1})	R^2	Exp. q_e (mg g^{-1})
3.12	0.194	0.9705	2.75
Intra-particle diffusion			
k_{id} (mg g^{-1} $min^{-0.5}$)	C (mg g^{-1})	R^2	
0.46	0.107	0.842	

3.6. Effect of temperature and thermodynamics studies.

Temperature, an important parameter in the adsorption process, is directly linked to the kinetic energy of the adsorbent in the solution. The influence of temperature on Be removal was investigated at a temperature range of 25-65°C. Figure 14 illustrates that the removal percentage decreased with increasing temperature. Therefore, 25°C can be considered as the optimum temperature for beryllium ions adsorption experiments.

The adsorption thermodynamic parameters provide a great deal of information concerning the type and mechanism of the adsorption process. Thermodynamic parameters associated with the adsorption, such as enthalpy change (ΔH), entropy change (ΔS), and Gibbs free energy change (ΔG) are calculated by the following equations [40]:

$$\Delta G = -RT\ln K_e \quad (14)$$

$$\ln K_e = \frac{\Delta S}{R} - \frac{\Delta H}{RT} \quad (15)$$

$$\Delta G = \Delta H - T\Delta S \quad (16)$$

Where K_e is the equilibrium constant, T is the absolute temperature (K), and R is the universal gas constant (8.314$Jmol^{-1}K^{-1}$). It appears from Eq. (15) that both ΔS and ΔH of sorption can be determined from the plot of ln K_e versus 1/T (Figure 15). The thermodynamic parameters are presented in Table 3. The negative values of ΔG indicate the feasibility and spontaneous nature of the adsorption process. The negative value of ΔH confirms that beryllium sorption is an exothermic process, while the positive value of ΔS shows an increase of the randomness during Be adsorption by the prepared EIR resin. Moreover, it may be related to the liberation of water from hydration during the adsorption process, causing an increase in the system's randomness [46].

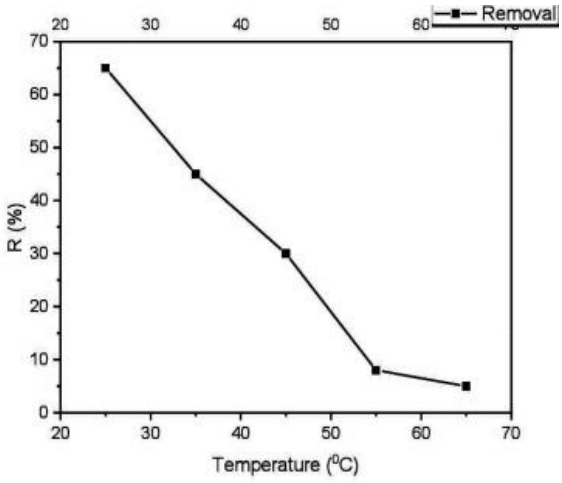

Figure 14. Effect of temperature on the removal Percentage of Be by EIR resin.

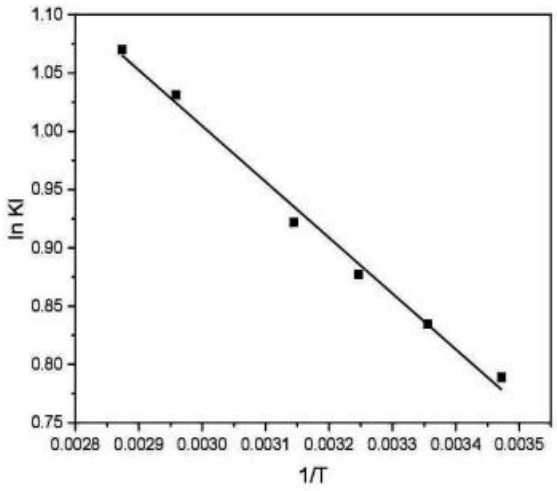

Figure 15. A plot of ln K_e versus 1/T for the determination of thermodynamic parameters

Table3. Thermodynamic parameters for the adsorption of Be by calcion/ XAD-2010.

Temp (°C)	ΔG (kJ mol^{-1})	ΔH (kJ mol^{-1})	ΔS (J mol^{-1} K^{-1})
25	-1.7		
35	-1.9		
45	-2.1	- 3.4	0.2
55	-2.4		
65	-2.7		

3.7. Desorption studies.

From the reusability point of view, the stability of EIR is of crucial importance, and the adsorbed metal ions should be easily desorbed without destroying the EIR under operation conditions. To find the convenient eluent for desorption of the metal ions from the EIR resin, different types of acid solutions, including nitric, sulfuric, and hydrochloric acid, were examined at different concentration values. The treatments involved stirring aliquots of 25ml solutions of metal ions with 0.05g of EIR resin for 25min at room temperature. Among the tested eluents, we deduce that 1.5M HCl achieved the maximum elution efficiency (95%) of Be ions. Therefore, 1.5M HCl solution was selected as an eluent for elution EIR resin.

4. Application

Finally, to assess the feasibility of EIR resin (calcion/XAD-2010) as the adsorbent for removing Be ions from the waste samples, adsorption experiments were carried out under the optimum conditions (pH 3.5, 25min contact time at room temperature). The waste sample was derived from the beryllium extractant project, Nuclear Materials Authority, Egypt. The obtained result indicated the effective removal of Be species from the derived waste sample.

Finally, to ensure the precise elimination of Be ions from the waste sample, the interfering ions were effectively masked by 2ml of 5% EDTA-2Na during the sorption process.

5. Conclusions

In the present study, batch adsorption experiments were carried out to remove Be from aqueous solutions using calcion/Amberlite XAD-2010 resin. The removal process was highly pH dependent, and the best results were obtained at a pH range of 3.0- 5.0. The equilibrium time for the sorption of Be was achieved within 25 minutes of contact time. Sorption isotherm and thermodynamic studies indicated the monolayer, exothermic, and spontaneous nature of

Be sorption by the EIR. Kinetic sorption data suggested the applicability of the pseudo-second-order kinetic model for the sorption process. The loaded Be ions on the investigated EIR resin was 2.75mg g^{-1}. The loaded resin was desorbed by 1.5M HCl. The obtained results evidenced the possibility of applying the impregnated resin to remove Be ions from the waste sample.

Funding

This research received no external funding.

Acknowledgments

Declared none.

Conflicts of Interest

The authors declare no conflict of interest.

References

1. Fouad, H.K.; Atrees, M.S.; Badawy, W.I. Development of spectrophotometric determination of beryllium in beryl minerals using chrome Azurol S. *Arab. Chem. J.* **2016,** *9*, S235-S239, http://doi.org/10.1016/j.arabjc.2011.03.012.
2. Bolan, S.; Wijesekara, H.; Tanveer, M.; Boschi, V.; Padhye, L.P.; Wijesooriya, M.; Wang, L.; Jasemizad, T.; Wang, C.; Zhang, T.; Rinklebe, J.; Wang, H.; Lam, S.S.; Siddique, K.H.M.; Kirkham, M.B.; Bolan, N. Beryllium contamination and its risk management in terrestrial and aquatic environmental settings. *Environ. Pollut.* **2023**, *320*, 121077, https://doi.org/10.1016/j.envpol.2023.121077.
3. Burkhardt, F.; Pieralli, S.; Bergfeldt, T.; Wemken, G.; Wesemann, C.; Stolz, D.; Spies, B.C**.** Elemental analysis of contemporary dental materials regarding potential beryllium content. *Sci. Rep.* **2022**, *12*, 19119, https://doi.org/10.1038/s41598-022-21068-9.
4. Islam, M.R.; Sanderson, P.; Naidu, R.; Payne, T.E.; Johansen, M.P.; Fazle Bari, A.S.M.; Rahman, M.M. Beryllium in contaminated soils: Implication of beryllium bioaccessibility by different exposure pathways. *J. Hazard. Mater.* **2022**, *421*, 126757, https://doi.org/10.1016/j.jhazmat.2021.126757.
5. Arar, O. Removal of beryllium (Be2+) from water samples by sorption process: a review. *Water Water Purifi. Techno*. *Sci. Techni*. *News*. **2021**, *31*, 3-11, https://doi.org/10.20535/2218-930032021244564.
6. Hassan, J. Green solid phase extraction for preconcentration of Beryllium in aqueous samples. *Anal. Chem.Indian J.* **2012**, *11*, 311-315.
7. Rezabeyk, S.; Manoochehri, M. Selective extraction and determination of beryllium in real samples using amino-5,8-dihydroxy-1,4-naphthoquinone functionalized magnetic MIL-53 as a novel nanoadsorbent. *RSC Adv.* **2020**, *10*, 36897-36905, http://doi.org/10.1039/d0ra05408a.
8. Atrees, M.S.; Mira, H.I.E.; Kawassik, Y.M.; Ali, M.E.M. Comparative Studies on Hydrometallurgy and Pyrometallurgy to the Extraction of Beryllium from Decrepitated Beryl from Wadi El Gemal Region, Eastern Desert, Egypt**.** *J. Phys.: Conf. Ser.* **2022,** *2305*, 012034, http://doi.org/10.1088/1742-6596/2305/1/012034.
9. El Hady, S.M.; Abdeldaym, S.M. A. Suggested Procedure for Chemical Processing of Beryl from Received Geological Sample, Eastern Desert, Egypt by Solvent Extraction Technique**.** *TIMS Acta* **2022**, *110*, 56-67, http://doi.org/10.21608/TIMS.2021.102029.1000.
10. Smithwick III, R.W.; Bowman Jr, D.W.; Oatts, T.J. Beryllium characterization in soils by selective extraction. *Talanta* ***2021***, *223*, 121742, https://doi.org/10.1016/j.talanta.2020.121742.
11. Tokarčíková, M.; Motyka, O.; Peikertová, P.; Gabor, R.; Seidlerová, J**.** Magnetically Modified Biosorbent for Rapid Beryllium Elimination from the Aqueous Environment. *Materials* **2021**, *14*, 6610, https://doi.org/10.3390/ma14216610.
12. Zhao, X.; Su, Y.; Lei, Z.; Wang, H.; Hu, E.; Hu, F.; Wang, Q.; Xu, L.; Fan, S.; Liu, X.; Hao, X. Adsorptive removal of beryllium by Fe-modified activated carbon prepared from lotus leaf. *Environ. Sci. Pollut. Res.* **2023,** *30*, 18340–18353, https://doi.org/10.1007/s11356-022-23415-9.

13. Metwally, E. Kinetic studies for sorption of some metal ions from aqueous acid solutions onto TDA impregnated resin. J. *Radioanal. Nucl. Chem.* **2006**, *270*, 559–566, https://doi.org/10.1007/s10967-006-0462-5.
14. Navarro, R.; Saucedo, I.; Núñez, A.; Ávila, M.; Guibal, E. Cadmium extraction from hydrochloric acid solutions using Amberlite XAD-7 impregnated with Cyanex 921 (tri-octyl phosphine oxide). *React. Funct. Polym.* **2008**, *68*, 557–571, https://doi.org/10.1016/j.reactfunctpolym.2007.10.027.
15. Seyhan, S.; Merdivan, M.; Demirel, N. Use of o-phenylene dioxydiacetic acid impregnated in Amberlite XAD resin for separation and preconcentration of uranium (VI) and thorium(IV*). J. Hazar. Mat.* **2008**, *152*, 79–84, https://doi.org/10.1016/j.jhazmat.2007.06.065.
16. Hosseini, M.S.; Hosseini-Bandegharaei, A. Selective extraction of Th(IV) over U(VI) and other co-existing ions using eosin B-impregnated Amberlite IRA-410 resin beads. *J. Radioanal. Nucl. Chem.* **2010**, *283*, 23–30, http://doi.org/10.1007/s10967-009-0037-3.
17. Kovalenko, O.; Baulin, V.; Baulin, D.; Tsivadze, A. Solvent-Impregnated Resins Based on the Mixture of (2-Diphenylphosphoryl)-4-ethylphenoxy)methyl) diphenylphosphine Oxide and Ionic Liquid for Nd(III) Recovery from Nitric Acid Media. *Molecules* **2021**, *26*, 2440, https://doi.org/10.3390/molecules26092440.
18. Bezhin, N.A.; Frolova, M.A.; Kozlovskaia, O.N.; Slizchenko, E.V.; Shibetskaia, I.G.; Tananaev, I.G. Physical and Chemical Regularities of Phosphorus and Beryllium Recovery by the Sorbents Based on Acrylic Fiber Impregnated by Iron Hydroxide (III). *Processes* **2022,** *10*, 2010, https://doi.org/10.3390/pr10102010.
19. Elci, L.; Soylak, M.; Dogan, M. Preconcentration of trace metals in river waters by the application of chelate adsorption on Amberlite XAD-4. *Fresenius J. Anal Chem.* **1992**, *342*, 175-178, https://doi.org/10.1007/BF00321717.
20. Abd El Fatah, A.I.L.; Elashry, S.M. La (III) Separation by Tri Octyl Phosphine Oxide (Cyanex 921) Based on Amberlite Xad-4 Chelating Resin. *J. Inorg. Organomet. Polym.* **2022,** *32*, 2793- 2805, https://doi.org/10.1007/s10904-022-02344-7.
21. Saleh, M. A. Chemical studies on the estimation of beryllium in ores and rocks. M. Sc. Thesis, Menoufia Univ., Egypt, **1999**.
22. Blaz, T.; Migdalski, J.; Lewenstam A. Polypyrrole–calcion film as a membrane and solid-contact in an indicator electrode for potentiometric titrations. *Talanta* **2000**, *52*, 319–328, http://doi.org/10.1016/s0039-9140(00)00363-5.
23. Fouad, H.; Elenein, S.A.; Orabi, A.; Abdulmoteleb, S. A new extractant impregnated resin for separation of traces of uranium and thorium followed by their spectrophotometric determination in some geological samples. *SN Appl. Sci.* **2019,** *1*, 309, https://doi.org/10.1007/s42452-019-0325-7.
24. Narkesabad, Z.S.; Rafiee, R.; Jalilnejad, E. Experimental study on evaluation and optimization of heavy metals adsorption on a novel amidoximated silane functionalized *Luffa cylindrical*. *Sci. Rep.* **2023**, *13,* 3670, https://doi.org/10.1038/s41598-023-30634-8.
25. Elabd, A.A.; Zidan, W.I.; Abo-Aly, M.M.; Bakier, E.; Attia, M.S. Uranyl ions adsorption by novel metal hydroxides loaded Amberlite IR120. *J. Environ. Radioact.* **2014**, *134*, 99-108. http://doi.org/10.1016/j.jenvrad.2014.02.008.
26. Cortina, J.L.; Miralles, N.; Aguilar, M.; Sastre, A.M. Extraction studies of Zn(II), Cu(II) and Cd(II) with impregnated and Levextrel resins containing di(2-ethylhexyl) phosphoric acid (Lewatit 1026 Oc). *Hydrometallurgy* **1994**, *36*, 131-142, https://doi.org/10.1016/0304-386X(94)90001-9.
27. Anirudhan, T.S.; Rijith, S. Synthesis and characterization of carboxyl terminated poly(methacrylic acid) grafted chitosan/bentonite composite and its application for the recovery of uranium(VI) from aqueous media. *J. Environ. Radioact.* **2012**, *106*, 8–19, https://doi.org/10.1016/j.jenvrad.2011.10.013.
28. Basaki, N.; Kakanejadifard, A., Shabanian, M.; Faghihi, K. Synthesis and characterization of a new photosensitive and electroactive polyamide/LDH nanocomposite containing azo groups. *Polym. Bull.* **2020**, *77*, 6433-6448, https://doi.org/10.1007/s00289-019-03048-8.
29. Doan, T.H.Y.; Pham, H.A.; Nguyen, N.H.; Le, T.D.; Nguyen, T.B.; Le, T.S. Adsorptive Removal of Azo Dye New Coccine Using High-Performance Adsorbent-Based Polycation-Modified Nano-Alpha Alumina Particles. *J. Anal. Methods Chem.* **2022**, *2022*, 9425334, https://doi.org/10.1155/2022/9425334.
30. Baba, A.A.; Olaoluwa, D.T.; Balogun, A.F.; Ibrahim, A.S.; Olasinde, F.T.; Adekola, F.A.; Ghosh, M.K. Extraction equilibrium conditions of beryllium and aluminium from a beryl ore for optimal industrial beryllium compound production. *Can. Metall. Q.* **2019**, *58*, 232-240, https://doi.org/10.1080/00084433.2018.1535930.

31. Schmidbaur, H. Recent contributions to the aqueous coordination chemistry of beryllium. *Coord. Chem. Rev.* **2001**, *215*, 223-242, http://doi.org/10.1016/S0010-8545(00)00406-9.
32. Erdem, E.; Karapinar, N.; Donat, R. The removal of heavy metal cations by natural zeolites. *J. Colloid Interface Sci.* **2004**, *280*, 309-314, https://doi.org/10.1016/j.jcis.2004.08.028.
33. Gupta, S.S.; Bhattacharyya, K.G. Immobilization of Pb(II), Cd(II) and Ni(II) ions on kaolinite and montmorillonite surfaces from aqueous medium. *J. Environ. Manage.* **2008**, *87*, 46–58, https://doi.org/10.1016/j.jenvman.2007.01.048.
34. Kılınçarslan, R.; Erdem, E.; Kocaokutgen, H. Synthesis and spectral characterization of some new azo dyes and their metal complexes. *Transition Met. Chem.* **2007**, *32*, 102-106, http://doi.org/10.1007/s11243-006-0134-x.
35. Hosseini, M.S.; Hosseini-Bandegharaei, A.; Raissi, H.; Belador, F. Sorption of Cr(VI) by Amberlite XAD-7 resin impregnated with brilliant green and its determination by quercetin as a selective spectrophotometric reagent. *J. Hazar. Mater.* **2009**, *169*, 52–57, https://doi.org/10.1016/j.jhazmat. 2009. 03.058.
36. Lu, L.; Na, C. Gibbsian interpretation of Langmuir, Freundlich and Temkin isotherms for adsorption in solution. *Philos. Mag. Lett.* **2022,** *102*, 239-253, https://doi.org/10.1080/09500839.2022.2084571.
37. Ghodbane, I.; Hamdaoui, O. Removal of mercury(II) from aqueous media using eucalyptus bark: Kinetic and equilibrium studies. *J. Hazard. Mater.* **2008**, *160*, 301–309, http://doi.org/10.1016/j.jhazmat.2008.02.116.
38. Freundlich, H.M.F. Over the Adsorption in Solution. *J. Phys. Chem.* **1906,** *57*, 385-471.
39. Ragadhita, R.; Nandiyanto, A.B.D. How to Calculate Adsorption Isotherms of Particles Using Two-Parameter Monolayer Adsorption Models and Equations. *Indones. J. Sci. Technol.* **2021**, *6*, 205-234, http://doi.org/10.17509/ijost.v6i1.32354.
40. Foo, K.Y.; Hameed, B.H. Insights into the modeling of adsorption isotherm systems. *Chem. Eng. J.* **2010**, *156*, 2-10, http://doi.org/10.1016/j.cej.2009.09.013.
41. Chu, K.H. Revisiting the Temkin Isotherm: Dimensional Inconsistency and Approximate Forms. *Ind. Eng. Chem. Res.* **2021**, *60*, 13140-13147, https://doi.org/10.1021/acs.iecr.1c01788.
42. Hutson, N.D.; Yang, R.T. Theoretical basis for the Dubinin–Radushkevitch (D–R) adsorption isotherm equation. *Adsorption* **1997**, *3*, 189-195, https://doi.org/10.1007/BF01650130.
43. Lagergren, S. About the Theory of So-Called Adsorption of Soluble Substances. Kungliga Svenska Vetenskapsakademiens Handlingar **1898**, *24*, 1–39.
44. Ho, Y.S.; McKay, G. Pseudo-second order model for sorption processes. *Process. Biochem.* **1999**, *34*, 451-465, https://doi.org/10.1016/S0032-9592(98)00112-5.
45. Weber Jr., W.J.; AM.ASCE; Morris, J.C. Kinetics of Adsorption on Carbon from Solution. *J. Sanit. Eng. Div.* **1963**, *89*, 31–59, https://doi.org/10.1061/JSEDAI.0000430.
46. Hosseini-Bandegharaei, A.; Hosseini, M.S.; Jalalabadi Y., Sarwghadi M.; Nedaie, M.; Taherian, A.; Ghaznavi, A.; Eftekhari, A. Removal of Hg(II) from aqueous solutions using a novel impregnated resin containing 1-(2-thiazolylazo)-2-naphthol (TAN). *Chem. Eng. J.* **2011**, *168*, 3, 1163-1173, https://doi.org/10.1016/j.cej.2011.02.004.